

A low-cost unity-based virtual training simulator for laparoscopic partial nephrectomy using HTC Vive

Fareeha Rasheed¹, Faisal Bukhari^{Corresp., 1}, Waheed Iqbal¹, Muhammad Asif², Hafiza Ayesha Hoor Chaudhry³

¹ Department of Data Science, University of the Punjab, Lahore, Pakistan

² Department of Computer Science, National Textile University, Faisalabad, Pakistan

³ Department of Computer Science, University of Turin, Piedmont, Italy

Corresponding Author: Faisal Bukhari
Email address: faisal.bukhari@pucit.edu.pk

Laparoscopic education and surgery assessment increase the success rate and lower the risks during actual surgeries. Hospital trainees require a safe and controlled environment, with affordable resources to practice and enhance their laparoscopic skills. Thus we have modeled and developed a surgical simulator to provide the initial training in Laparoscopic Partial Nephrectomy (LPN - a procedure to treat kidney cancer or renal masses). For this purpose, we have utilized an open-source game engine to develop a virtual simulator that can be accessed with a commercially available low-cost virtual reality (VR) device for visual and haptic feedback. The novel simulation with a soft body deformation based on simplex meshes can run efficiently on both CPU and GPU-based machines. This study shows the design of the proposed simulator, compares the cost, and evaluates the simulator performance using face and content validity measures. The controlled soft body effect, physics-based deformation, and haptic rendering using the HTC Vive provide the benefits of a good surgical simulator with a balanced trade-off between cost and performance. The experiments depict a positive feedback from the medical volunteers practicing initial LPN procedures for novice surgeons.

A Low-cost Unity-based Virtual Training Simulator for Laparoscopic Partial Nephrectomy using HTC Vive

Fareeha Rasheed¹, Faisal Bukhari¹, Waheed Iqbal¹, Muhammad Asif², and Hafiza Ayesha Hoor Chaudhry³

¹Department of Data Science, University of the Punjab, Lahore, Pakistan

²Department of Computer Science, National Textile University, Faisalabad 37610, Pakistan

³Department of Computer Science, University of Turin, Italy

Corresponding author:

Faisal Bukhari¹

Email address: faisal.bukhari@pucit.edu.pk

ABSTRACT

Laparoscopic education and surgery assessment increase the success rate and lower the risks during actual surgeries. Hospital trainees require a safe and controlled environment, with affordable resources to practice and enhance their laparoscopic skills. Thus we have modeled and developed a surgical simulator to provide the initial training in Laparoscopic Partial Nephrectomy (LPN - a procedure to treat kidney cancer or renal masses). For this purpose, we have utilized an open-source game engine to develop a virtual simulator that can be accessed with a commercially available low-cost virtual reality (VR) device for visual and haptic feedback. The novel simulation with a soft body deformation based on simplex meshes can run efficiently on both CPU and GPU-based machines. This study shows the design of the proposed simulator, compares the cost, and evaluates the simulator performance using face and content validity measures. The controlled soft body effect, physics-based deformation, and haptic rendering using the HTC Vive provide the benefits of a good surgical simulator with a balanced trade-off between cost and performance. The experiments depict a positive feedback from the medical volunteers practicing initial LPN procedures for novice surgeons.

1 INTRODUCTION

Renal cancer is among the top ten cancers in both males and females, though males have a double chance of developing it than the females (1). Since the discovery of open radical nephrectomy (ORN) in the 1960s, the surgical removal of tumors from kidney using open radical nephrectomy has been the cornerstone of treatment for confined renal cell carcinoma (RCC) (2; 3). In 1991, the first report of a minor renal tumor treated with laparoscopic radical nephrectomy (LRN) was published after which it was widely-accepted as the new standard procedure for surgical recession of renal cancer (4). In laparoscopic Nephrectomy the surgeon makes a small incision on the patient's body and glides the laparoscopic instrument inside the body cavity. The extraction of renal tumor is performed inside the body cavity using a small camera to guide the surgeon of the surrounding organs. Laparoscopic nephrectomy (LPN) is safer, quickly recoverable (as a result of the small cut), and produces better outcomes than the conventional open radical surgery. Laparoscopic nephrectomy also requires exceptional hand-eye coordination, a lot of surgical practice along with technical training, making it a more difficult surgical procedure with a steep learning curve as compared to open radical nephrectomy (5; 6). Owing to these reasons, laparoscopic nephrectomy is still harder to adapt as the standard practice in developing countries.

To solve these problems, virtual reality is used. Virtual reality not only enables distance learning and training in the medical field but also provides a suitable alternative to in-vivo surgeries (15). The virtual realistic laparoscopic simulator enables surgeons to rehearse various laparoscopic techniques, including clipping, cutting, suturing, knot tying, and camera handling (7; 8). By virtue of these laparoscopic

46 practices using advanced imaging and surgical techniques, the post surgery results in reduced hospital
47 stays and a faster recovery rate. It also ensures a less painful surgery with little blood loss and improved
48 cosmetic results.

49 There are various types of virtual reality simulators available in the market nowadays. Most simulators'
50 ultimate goal is to present training systems that can prepare surgeons for complex operations in advance
51 (9; 10). The field of laparoscopic training, skill assessment, and haptic feedback is well researched
52 (11; 12; 13). However, there is still a need for improvement in low-cost hardware systems with trainees'
53 evaluation for developing and underprivileged counties. These systems as shown to serve as an investment
54 to enhance the surgical skills of doctors using game-based training (14; 16). It also increase the trainees
55 self-confidence, skills, and experience in a controlled and repeatable environment tackling the moral issue
56 of practicing on other living-beings (17; 18; 19). Some studies explicitly highlighted the importance and
57 key benefits of using Unity for real-time applications and simulation purposes (20; 21). The HTC Vive
58 VR device is getting attention as a low-cost simulation tool for its high accuracy and precision in position
59 tracking. It is considered suitable for experiments that do not require self-motion, thus proving it a good
60 option for surgery training (22; 23).

61 In this study, we present a low-cost surgical Unity-based Virtual Training Simulator for laparoscopic
62 partial nephrectomy using HTC Vive. The main contributions of our research work are:

- 63 1. Creation of an anatomical model for the kidney with Renal Cell Carcinoma (RCC) and minimal
64 mesh representation.
- 65 2. Proposing a stable and efficient solution for soft body deformation using Position Based Dynamics
66 (PBD) combined with the force-based method.
- 67 3. Using a game engine when developing a specialized LPN training environment for surgeons.
- 68 4. Exploring the possible use of a low-cost HTC Vive VR device for training purposes and haptic
69 feedback.
- 70 5. Determining the validity measures for our simulator and criterion-based approach for surgeons'
71 evaluation.

72 Compared with other high fidelity expensive trainers, our proposed training system based on Unity
73 follows a more straightforward deformation representation with less computing time but high solving
74 speed. Compared to the previous methods, the flexibility of the proposed algorithm in tuning the
75 parameters allows users to have great control over the simulation. The user can easily visualize and
76 interact with the deforming body using the HTC Vive HMD and controllers.

77 **1.1 Details and Challenges in LPN**

78 LPN has emerged as a viable alternative to open nephrectomy while minimizing patient morbidity. The
79 advancements in laparoscopic experience have helped treat exophytic renal tumors, which is the main
80 focus of this study.

81 The Da Vinci Surgical System is usually used for surgical practices as it is safe and very accurate.
82 However the machine is very costly. Fig. 1 is added here to show the typical surgical procedure of Da
83 Vinci surgical system. This procedure usually requires four primary steps: a) position the patient in the
84 right place and insert the camera and other instrumentation through the trocars; b) dissect the tissues to
85 find the exact location of the tumor, vessels, and the ureter; c) clip and ligate the kidney structure; d)
86 tease away adhesions between the kidney and tumor part and suture the saved part of the kidney. Our
87 team has simulated some of the same steps with a simple mesh representation and rendered them over the
88 HTC Vive, which is much cheaper than the Da Vinci machines. Our system can be made available to
89 surgeons in developing countries for an initial LPN practice at a very affordable rate. We have focused on
90 the essential steps b) and d) of Fig. 1, as others can be practiced in separate training sessions.

91 The main difficulties during the operating process that require practice are:

- 92 1. Identifying the exact tumor location is necessary to save the kidney and surrounding parts from
93 unnecessary damage.
- 94 2. Clipping the renal artery, renal vein, and ureter helps prevent uncontrollable bleeding.

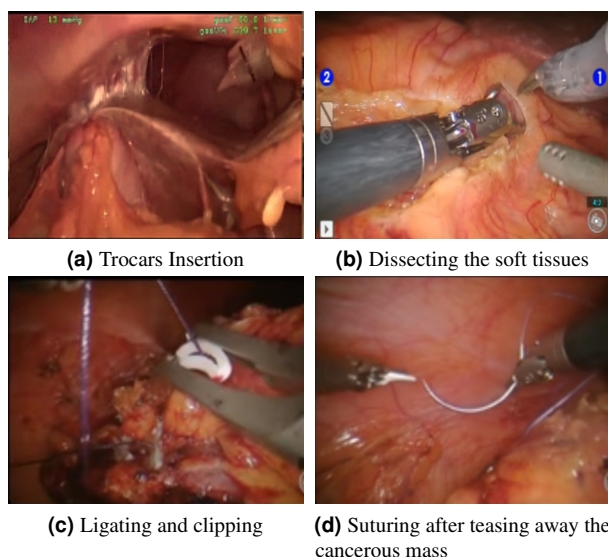


Figure 1. Core steps of a surgical procedure. Reprinted from (24).

- 95 3. Correctly separating adhesions among the kidneys can prevent procedure failure.
- 96 4. The laparoscopic instrument insertion should be performed carefully as unskilled manipulation can
- 97 damage the main blood vessels and intestines.

98 The ability to handle this wide range of indications will allow the surgeon to efficiently practice and

99 perform a wide range of partial nephrectomies.

100 2 RELATED WORK

101 Yu et al. (25) have analyzed the literature on partial nephrectomy to put the diagnosis and treatment of

102 renal cancer in a modern context. This procedure has the main advantage of preventing complete kidney

103 loss, but the drawbacks include the potential for regional infection and other complications. In their

104 research, Verhoest et al. (26) have discussed some of the effects of laparoscopic nephrectomy compared

105 to open nephrectomy for the disease of Autosomal Dominant Polycystic Kidney Disease (ADPKD). They

106 identified that the incisional hernias occurred in two patients who had open cyst removal. In contrast,

107 there was minimal blood loss, less postoperative pain, and rapid recovery with laparoscopic nephrectomy.

108 Christian et al. (27) have discussed some of the algorithms and techniques for surgical modelling of

109 tissues and blood vessels so that these models can be effectively used while training. Another exciting

110 research work of Qian et al. (28) has focused on the efficient methods of computation and simulation

111 frameworks instead of individual issues of deformation, force direction, and feedback. The techniques

112 offered have many intuitive parameters for realistic rendering. The tailored algorithms in these works

113 (29; 30) based on the finite element method (FEM) and extended finite element method (XFEM) suggest

114 improvements for the efficiency of simulation and accuracy of the designed procedure. However, the

115 FEM method usually requires a longer execution time and a more extensive data set for mapping nodal

116 connectivity. The position-based dynamics (PBD) method is more convenient and stable due to nonlinear

117 constraint handling, and a fast convergence rate (31; 32). It directly manipulates the vertex positions,

118 omitting the velocity layer as opposed to the FEM method. Another helpful approach is extended position-

119 based dynamics (XPBD), which implicitly provides force estimates, making simulations visually look

120 realistic but requiring high processing power (33).

121 Witt et al. (34) have highlighted the three soft tissue deformation techniques: linear elasticity theory,

122 tensor-mass model, and spring-mass model. The computational complexity of all models depends on the

123 number of edges involved. They developed a new hybrid technique featuring the benefits of previous

124 tissue cutting and tear modelling methods. Many state-of-the-art works use the SOFA architecture for

125 simulations. It incorporates hyperelasticity with realistic object physics, which is computationally more

126 intensive. It works well with haptic devices like Geomagic, ARTTrack, Novint, Falcon, etc. (35). The
 127 advancements and growing requirements in the simulation of virtual healthcare environments require a
 128 change in the development process. The development process must decrease the method's complexity and
 129 trainer expenses.

130 To increase the surgical ability among surgeons, low-cost virtual devices are being implemented,
 131 thus increasing market competition. To find a cost-effective solution and limit the problems related to
 132 the controlled training environment, Zhong et al. (36) and Wheeler et al. (37) have developed plausible
 133 virtual environments using Unity3D. The game engines help with fast prototyping and response collection.
 134 Nowadays, different commercially available head-mounted displays are used in specific scenarios, and
 135 their performance is evaluated based on the type of functionality they provide (38; 39). In their study,
 136 Vamadevan et al. (40) have discussed the use of haptic and non-haptic responsive devices as the most
 137 effective means to acquire surgical training with a sense of realism in comparison to old-school methods.
 138 This study compared different simulators based on their working technology, response to external forces,
 139 degree of freedom, authenticity, and immersive experience. In this study (41), Nemani et al. used the task
 140 performance scores as assessment metrics for the Fundamentals of Laparoscopic Surgery (FLS) trainers
 141 and the Virtual Basic Laparoscopic Skill Trainer (VBLaST) trainers of a pattern cutting simulator.

142 There is an enormous gap to close for improvements in accurate functioning, effective organ modeling,
 143 less computational time, and standardization of metrics used for surgeons' evaluation. The critical point
 144 is the ongoing evaluation of existing systems and the establishment of specific practise tasks, scores, and
 145 training time as directed by these works (42; 43).

146 This study focuses on the efficient method of soft body modeling, position-based mesh deformation,
 147 performance evaluation in terms of stability and quick solving time, and haptic feedback from the system
 148 using a less expensive VR device. Similarly, by simulating the virtual environment through Unity, we
 149 have studied this game engine's capacities and limitations, focusing on the training purpose. Other works
 150 mentioned do not consider using the HTC Vive as a surgical trainer.

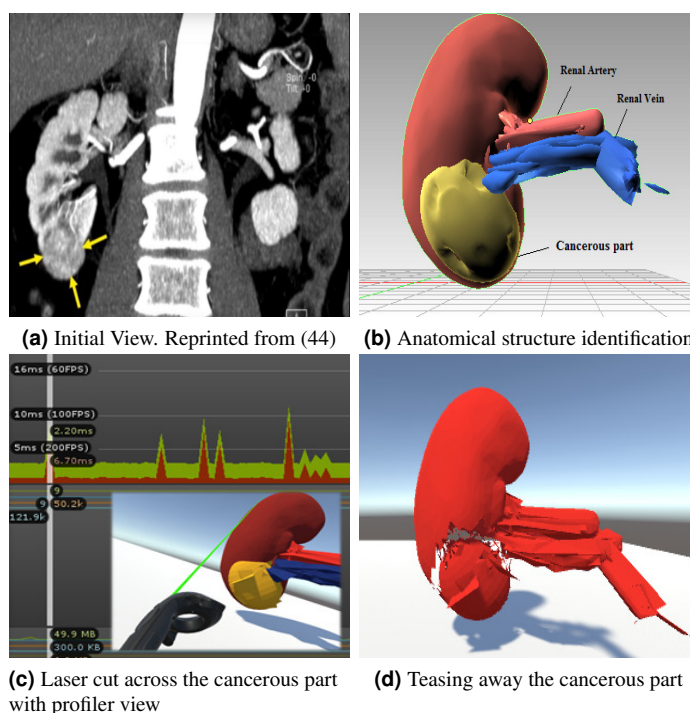


Figure 2. Modular views of laparoscopic partial nephrectomy simulated procedure.

151 3 SYSTEM INFRASTRUCTURE

152 Usually, a training simulator consists of a rendering component for viewing 3D elements, the user
 153 interfaces for interaction, a physical element for practicing the procedure, and an event management

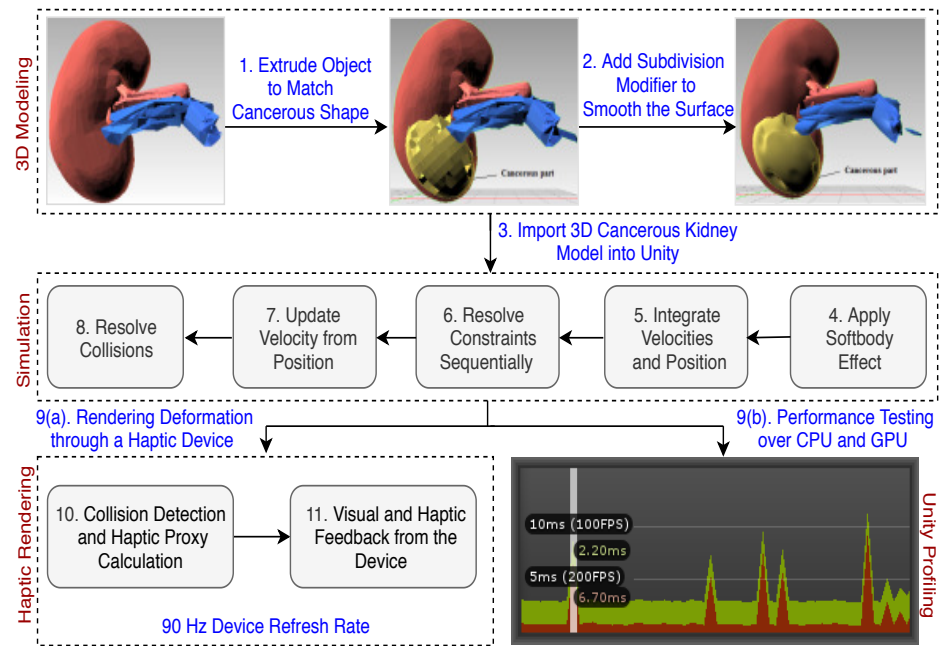


Figure 3. Laparoscopic partial nephrectomy system architecture.

154 module for input/output. Our simulator is based on the same hierarchy.

155 In our design component, we prototype a small renal cell carcinoma case with a peripheral mass of
 156 almost 3-5 cm. In practical terms, we construct the game module as below (Fig. 2 shows four primary
 157 steps):

- 158 1. A video (45) shows the process by which the insertion points are labeled and trocars inserted
 159 through the abdomen. The user can adjust the camera position to get the optimal viewpoint for his
 160 convenience.
- 161 2. The trainees are then required to identify cancerous tissues and other relevant structures.
- 162 3. With the help of two laser emitting controllers, trainees can easily mark and precisely cut along
 163 the cancerous structure, avoiding damage to the nearest tissues. The Unity profiler will record the
 164 task's performance time.
- 165 4. The final step is to tease away the cancerous part from the kidney.

166 4 SYSTEM DESIGN AND PHYSICAL SIMULATION

167 The soft body for kidney organs has been designed using Blender (46), and the physics behavior is
 168 interpreted through the Unity physics engine. The rendering process features the physical appearance of
 169 the object while cutting triangular meshes with a specific force in a particular direction. Fig. 3 represents
 170 an abstract view of the complete system architecture.

171 4.1 3D Modeling

172 We have modelled the kidney and cancerous part with simplex meshes, which are topologically dual
 173 triangulations. These meshes are more adaptive, depending on the local energy. This technique is widely
 174 used for efficient physics-based modeling. It permits efficient and robust object deformation.

175 **Joining Components:** Fig. 4 shows the kidney model consisting of different 3D components (renal
 176 artery, vein, and cancerous part) extruded and then joined together using Blender's Join operation. A
 177 subfigure (a) and (b) of Fig. 4 present the 3D structure of a healthy kidney with a solid and wireframe
 178 view, respectively. Relevant materials have been applied to match the organ color scheme and gain a better
 179 understanding. After incorporating the cancerous part on the mesh surface, a solid view in subfigure (c)

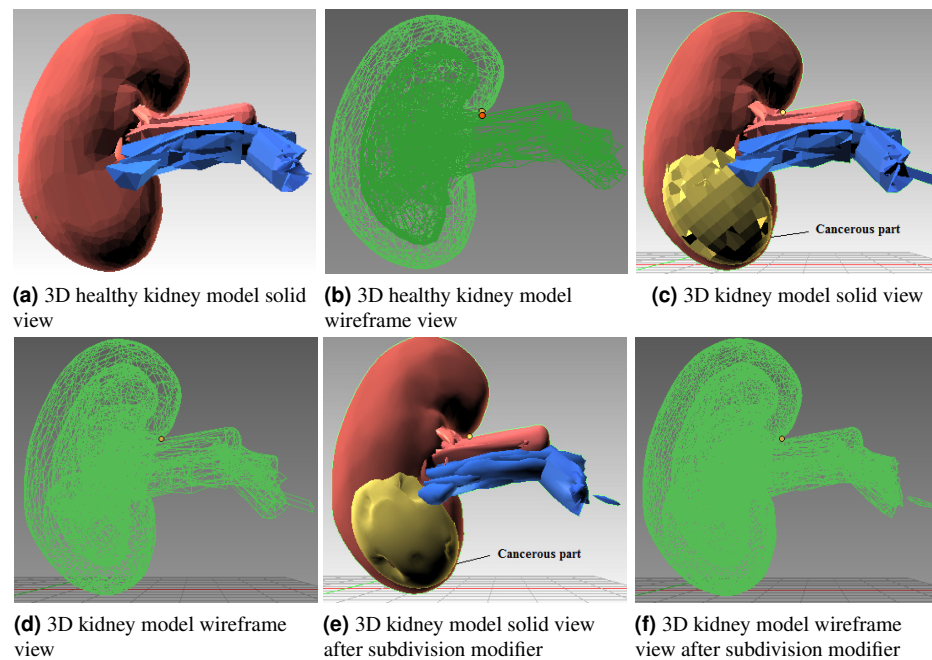


Figure 4. Step-wise 3D modeling of kidney organ and cancerous structure.

180 and a wireframe view in (d) of Fig. 4 can be seen. The rocky mesh surface in (c) is not plausible as the
 181 mesh triangles are sparse enough.

182 **Subdivision Modifier:** A subdivision surface modifier has been applied to the mesh surface to make
 183 it look smooth, which works by dividing the mesh triangles into subsurfaces. The basic topology of the
 184 mesh remained the same; just some of the properties were adjusted. The subfigure (e) and (f) of Fig. 4
 185 show the models after applying the modifier. Now the same surface area covers more triangles, which
 186 appear to be more delicate and smooth. This smooth structure is computationally heavy on the system
 187 as the CPU or GPU has to process more triangles than the model (c). We selected the model in (c) for
 188 simulation purposes as it's a trade-off between the computational cost and the visually realistic model.

189 4.2 Force based Soft Body Simulation

190 For this specific technique, a triangular mesh defines the structure of the soft body, and the constraints
 191 apply the necessary force to present the volumetric effect. Each surface point is modelled on account of
 192 forces like spring force, damping force, pressure force, and offset directional force. These forces exhibit
 193 the pressure on a particular region while the total number of vertices remains the same. The combined
 194 effect of these forces gives a subtle soft body effect, as the whole object would shift without changing its
 195 native structure.

196 We define the 3D soft body, SB3D, as

197 $SB3D = \{ S, F, V, N, C \}$

198 whereas S here defines the soft body,

- 199 • $F = \{ F_j \mid j = 0, \dots, m - 1 \}$ represents the set of forces for each point j.
- 200 • $V = \{ V_j \mid j = 0, \dots, m - 1 \}$ represents the set of velocities for each point j.
- 201 • N represents the count of total edges.
- 202 • C represents a constraints set being observed for object deformation.
- 203 • C represents a constraints set being observed for object deformation.

204 **Combined Force Effect:** The composite force, F_j is centered on elasticity control force, pressure
 205 control force, damping control force, and a direction offset component from the point j on the body. The
 206 composite force F_i is defined by the Equation (1) as:

$$F_j = F_{sj} + F_{dj} + F_{pj} + F_{oj} \quad (1)$$

207 where

- 208 • F_{sj} represents the spring force at point j,
- 209 • F_{dj} represents the damping force at point j,
- 210 • F_{pj} represents the pressure force at point j, and
- 211 • F_{oj} represents the offset force at point j.

212 Consider this simulation system with the numerical integration of Hooke's spring force described
213 through Equation (2).

$$F_j = m_j \cdot \frac{\partial^2 \vec{r}_j}{\partial t^2} \quad (2)$$

214 The pressure force applied will deform the body shape acting in the direction of normal vector \hat{n} as
215 described in the Equation (3).

$$P = \vec{P} \cdot \hat{n} \left[\frac{N}{m^2} \right] \quad (3)$$

216 Where P is a pressure value and \hat{n} , is a normal vector to the surface on which pressure force is acting.
217 For calculating specific pressure forces, we multiplied pressure by the surface area, giving us Equation
218 (4).

$$\vec{F}_p = \vec{P} \cdot \Delta A [N] \quad (4)$$

219 The algorithmic part 1 represents the soft body functioning of this model.

Result: Soft body effect

1. *Initialization*
2. *Loop over all particles:*
UpdateVertex(int)
3. *Loop over all faces:*
 - (a) UpdateVertexVelocity(vertex velocity)
 - (b) AddPressureForce(3D vertices, force)
 - (c) AddDeformingForce(3D vertices, force)
 - (d) AddForceToVertex(int, 3D vertices, force)

Algorithm 1: Force Based Soft Body Algorithm

220 **Detecting User Input:** A ray is tossed into the scene from the camera location. The physics engine of
221 Unity processes the location information of the object it hits. After clicking the controller trigger buttons,
222 we move over the mesh surface to place a cut along the triangles, capturing the location of points. Adding
223 the combined force at the contact points gives an elastic effect. Each surface point experiences a drag
224 force until it returns to its original position, as expressed by Equation (5).

$$v_d = v(1 - d\Delta t) \quad (5)$$

225 For a high value of damping force, the mesh becomes less bouncy. Spring and damping force scripted
 226 variables have been shown in part (a) of Fig. 5. The values for these variables can be easily changed, so
 227 the user may have complete control over how firm the generated soft body effect will be.

228



Figure 5. Mesh deformer input attached to scene camera.

229 **Moving Vertices Under the Pressure Force:** The function `AddPressureForce()` loops through all
 230 newly located points and adds the necessary pressure force separately. We can add a small direction offset
 231 in this loop so that the vertices are always driven into the surface, following the normal to the contact
 232 points. Pressure and offset force variables are shown in part (b) of Fig. 5.

233 Through Equation (6), we can find the exact distance between vertices and the direction in which
 234 force is applied.

$$F_v = \frac{F}{1 + d^2} \quad (6)$$

235 One plus the squared distance ensures the full-force strength even if the distance is zero. Once we
 236 know the force, we can use the relation $F = \frac{m}{a}$ and $a = \frac{\Delta v}{\Delta t}$ to calculate the approximate change in velocity.
 237 Considering the mass $m = 1$ for each vertex, we finally have the Equation (7).

$$\Delta v = F \Delta t \quad (7)$$

238 The vertices can now be shifted with an absolute velocity, updated with each frame. After that, the
 239 relocated vertices are added to the mesh to change its shape. We need to recalculate the normals for the
 240 newly located vertices. Each vertex position is adjusted by the Equation (8)

$$\Delta p = v \Delta t \quad (8)$$

241 **Dealing with Mesh Transformation:** We only have a set of vertices representing an elastic surface,
 242 but it does not have a real volume like solid real-world objects. While cutting, vertices begin to move as
 243 soon as we apply pressure on them with the specified spring and damping effect, which is further handled
 244 through collision and bending constraints in PBD. The mesh colliders for the kidney model do not get
 245 affected by these forces; that's why the natural shape of the object never changes while simulating.

246 4.3 Constraint Based Physics Approach

247 In PBD, model points are linked by the triangular edges of the mesh with common connection points.
 248 While simulating, the positions of the points and the direction of the force (velocity is always tangent,
 249 constraint force is still normal) are calculated directly. This is why the instability issues can be handled
 250 easily through PBD (30; 31). Equation (9) and Equation (10) provide the central idea of sequentially
 251 resolving the system with constraints of equality and inequality in different time steps.

$$C_j(x_{ij}, \dots, x_{in_j}) = 0 \quad (9)$$

$$C_j(x_{ij}, \dots, x_{in_j}) \geq 0 \quad (10)$$

252 While simulating, if one mesh triangle responds to the stretch amount in the direction normal to the
 253 force, the neighboring triangles will behave in response to bending constraints under the same stretching
 254 influence. The stretching constraint function is described for each connecting edge through Equation (11).

$$C_{\text{str}}(x_1, x_2) = |x_1 - x_2| - d_{12} \quad (11)$$

255 Where d_{12} is the length of the edge at rest position, the bending constraint generated for any two
 256 triangles is described through Equation (12).

$$C_{\text{bend}}(x_1, x_2, x_3, x_4) = \arccos(n_1 \cdot n_2) - \phi_{12} \quad (12)$$

257 where n_1 and n_2 represent the normal vectors in the rest position and ϕ_{12} is the dihedral angle between
 258 the triangle 1 and 2. The Equation (13) for minimizing the total energy defined as:

$$E_{\text{tot}} = \sum (k_{\text{str}} C_{\text{str}}^2 + k_{\text{bend}} C_{\text{bend}}^2) \quad (13)$$

259 where k_{str} and k_{bend} are global stiffness parameters.

Result: Constraints handling with collision detection

- 1: **forall** vertices i **do** GenerateCollisionConstraints ($x_i \rightarrow p_i$)
- 2: **loop** SolverIterations **times**
- 3: ProjectConstraints($C_1, \dots, C_n, P_1, \dots, P_m$)
- 4: **end loop**

Algorithm 2: Position Based Dynamics

260 The primary functioning of algorithm 2 is presented here: the solver iterations compute and project
 261 the position constraints. The calculated points are moved to their estimated locations, along with updating
 262 the point velocities. Distance constraints represent the connective part of the cancerous mass in the kidney.
 263 Each connection is breakable depending on the stiffness parameter and rest length. The marked points are
 264 torn apart by algorithms at a given break threshold. However, in our method, there is no simulation of
 265 fascia tissues, so the deformation is not visually plausible as it is just a single layer of a soft structure.
 266 When the cancerous component is separated from the kidney, the fascia looks like a broken piece of paper.
 267 Still, another considerable advantage is the reduced solving time due to the fewer mesh triangles.

268 4.4 Tactile Rendering and Force Feedback

269 The HTC Vive haptic device immerses the user with a strong sense of presence. The responsive haptic
 270 feedback improves cognition by providing consistent visual and sensory movement. The headset has a
 271 resolution of 1080×1200 per-eye, with a refresh rate of 90 Hz and a 110 degree field of view. The refresh
 272 rate is similar to most sensory devices, as shown in Fig. 6. However, we are enjoying a cost benefit here
 273 with the HTC Vive Pro VR device.

VR Devices	Oculus Rift S	HTC Vive Cosmos	Valve Index	Samsung HMD Odyssey+	Razer OSVR HDK	StarVR One
Refresh Rate	80 Hz	90 Hz	80 – 144 Hz	90 Hz	90 Hz	90 Hz

Figure 6. Refresh rate comparison of sensory devices (47).

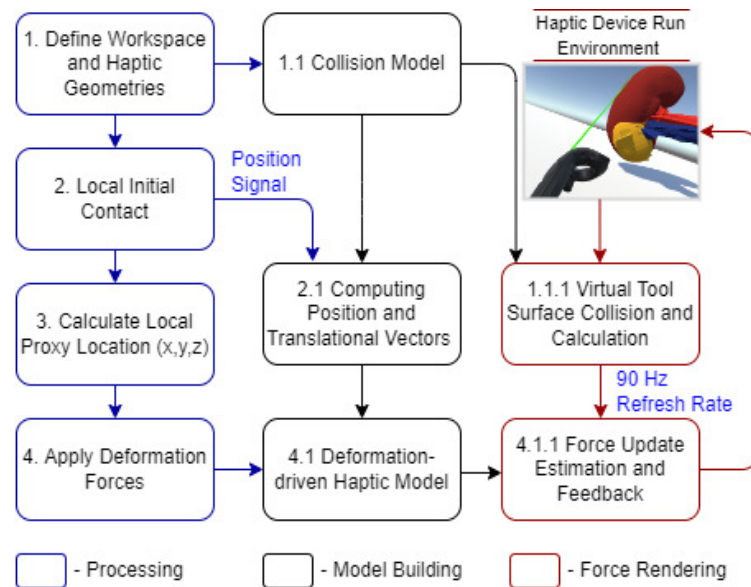


Figure 7. HTC Vive haptic device integrated workflow.

274 The SteamVR plugins in Unity allow us to manipulate haptic sensors in communication with organ
 275 tissues. Fig. 7 demonstrates the haptic device integrated workflow.

276 At first, the geometry track and initial contact information are processed. Then the haptic proxy
 277 continues to change along with the controller location. The fast refresh rate provides a plausible visual
 278 display of soft tissue deformation of a cancerous part. The PBD based collision model ensures stability
 279 while removing the triangular meshes from certain positions. This deformation gives visual feedback
 280 and an instant vibrational effect, which we have considered the haptic force feedback of the system. In
 281 this simulation scenario, the sensory device performance has been satisfactory while deforming the soft
 282 structure.

283 5 SYSTEM EVALUATION AND FEEDBACK

284 The Unity profiler has been used for evaluating system performance and usability. The Unity editor is
 285 good for fast profiling, as we do not have to release the application on the targeted platform for just testing
 286 purposes. This part discusses the experimentation and performance results obtained from the testing of
 287 the simulator on two different machines with different configurations.

288 5.1 Simulator Performance Comparison using Unity Profiler

289 The first simulation experiment was carried out on a system equipped with an Intel(R) Core(TM) i7-7700
 290 CPU running at 3.60 GHz, an x64-based processor, and 8.00 GB of installed memory. The second testing
 291 experiment has been performed using a high-end graphics system, the GeForce GTX 1060 with Max-Q
 292 Design 6.00 GB GDDR5 memory on the card, 1280 shading units, and 80 texture mapping units. This
 293 Max-Q design has the advantage of less power consumption as compared to other graphics cards.

294 Unity's "CPU/GPU Usage Profiler" displays data such as the time taken by different functions and
 295 events to get run, such as rendering, physics, animations, and scripts. This describes all the key areas
 296 where our system spends most of its time. The CPU usage for rendering the simulation has been shown
 297 at a specific timestamp in part (a) of Fig. 8 while part (b) of Fig. 8 shows the same simulating system
 298 rendering on the GPU, and we can see that most of the time is allocated to the "Game Player Loop" and
 299 its hierarchy.

300 Table 1 and Table 2 show the complete component details for Unity's renderer and memory profilers.

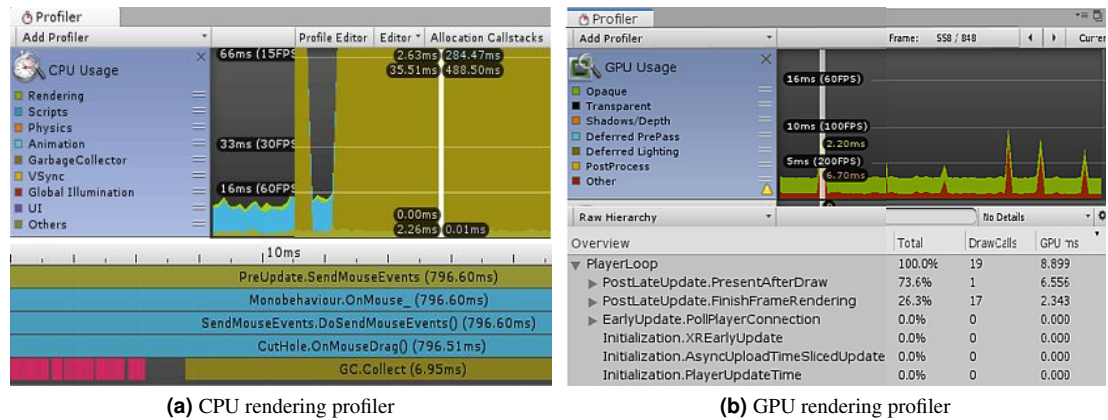


Figure 8. Screenshots from Unity Profiler rendering LPN simulation.

Rendering Parameters	CPU	GPU
Total Batches	19	9
Draw Calls	19	9
SetPass Calls	20	9
Triangles	50.2k	50.2k
Vertices	123.9k	121.9k
VRAM Usage	9.2MB	9.1MB

Table 1. CPU and GPU rendering profiler comparison.

Table 2. CPU and GPU memory profiler comparison.

Memory Parameters	CPU	GPU
Total Memory	38.9MB	49.9MB
Memory used by Unity	29.9MB	40.2MB
Textures	29/299KB	31/300KB
Meshes	11/6.8MB	6/6.8MB
Materials	24/79KB	26/87KB
Game Objects in a scene	14	16

301 GPU requires a high processing unit with a large amount of memory, which is quite expensive and
 302 hard to arrange by the hospital authorities when there will be a need for a large number of trainers. The
 303 computation time over the CPU was quite good with a short time step, but we had to compromise on the
 304 deformation performance, which was not plausible. The experience was much better with the GPU as it
 305 provides a parallel processing facility. Our simulation's overall computation time also decreased with a
 306 fast convergence rate.

307 5.2 Face and Content Validity for Simulator Performance Evaluation

308 To evaluate the overall performance and usability of the simulator, we have defined some face and content
 309 validity measures, as presented in Table 3 and Table 4. Each measure has a score range [0 - 9] (0 indicates
 310 a poor score, and 9 indicates an excellent score).

Table 3. Face validity measures for simulator performance evaluation.

Face Validity Measures
1. Realistic graphics
2. Precision of the platform
3. Instrument mapping
4. Anatomy representation
5. Interactivity of procedure

Table 4. Content validity measures for simulator performance evaluation.

Content Validity Measures
1. Useful for training novice surgeons
2. Useful for training expert surgeons
3. Useful for assessing cutting skills
4. Useful for assessing skill progression
5. Useful for assessing instrument handling

311 Seven final-year students and five interns from the department of nephrology at Shaikh Zayed Medical
 312 Complex Lahore voluntarily participated in this experiment. Subjects were given a brief explanation of
 313 the study's purpose and how to use the simulator. We are very thankful for their support here. A scoring
 314 system was assigned to each evaluation measure. The mean score values from both student and intern
 315 groups representing face and content validity measures are plotted in Fig. 9.

316

317 All participants found the simulated environment user-friendly and the HTC Vive haptic device helpful
 318 for increasing skill progression. We received positive feedback regarding the procedure interactivity and
 319 precision of the platform from both groups, as these measures reached the highest scores. The student
 320 group mentioned that realistic graphics should be improved. While performing the procedure, the intern
 321 group found instrument mapping to be ineffective. For simulation purposes, we have considered the laser
 322 pointer as the laparoscopic instrument.

323

324 Both groups agreed that the simulator is not in a position to train any expert surgeons yet. However,
 325 it possesses the ability to improve the tissue cutting skills of novice surgeons. More advanced testing
 326 techniques and measures will be used in the future to get more precise results. We intend to enhance the
 anatomy, force feedback, and simulator design and stability under the guidance of medical experts.

327 **5.3 Game based System Advantages and Limitations**

328 Using a constraint-based approach like PBD in combination with Unity has given us considerable
 329 advantages, along with some limitations.

330 **5.3.1 Advantages**

331

332 1. The constraint-based approach provides the solution to the instability problem. This method
 provides control and supports physical-based effects.

333

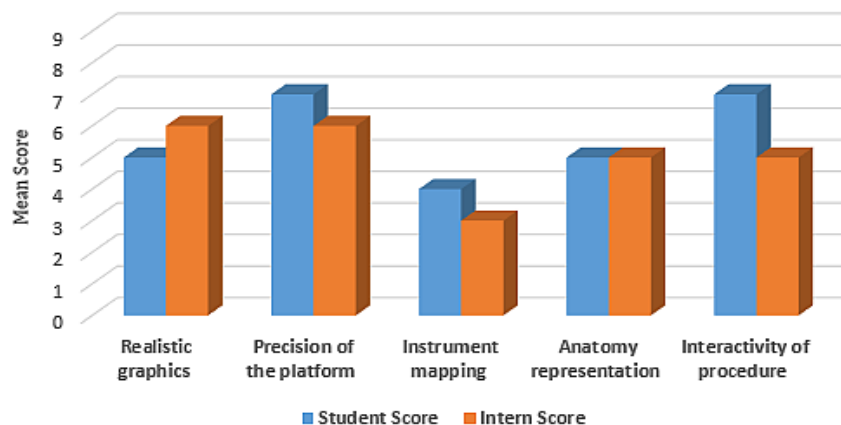
334 2. The point's positions and velocities are updated through a time-step method, so the overall compu-
 tational time gets decreased.

335

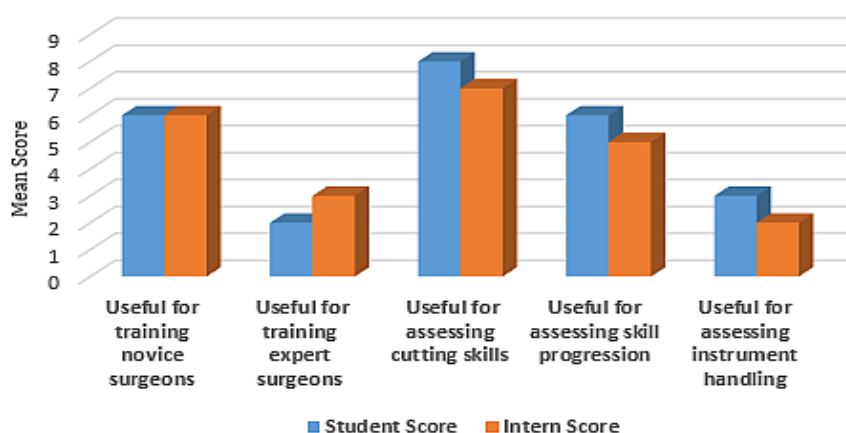
336 3. Game-based simulators are less expensive and help in fast prototyping, with a bit of compromise in
 functionality.

337

338 4. Modern game engines like Unity provide a user-friendly environment for simulating medical
 procedures, collaborative tasks, and emergencies.



(a) Mean score from student and intern group for face validity measures (0-Poor, 9-Excellent)



(b) Mean score from student and intern group for content validity measures (0-Poor, 9-Excellent)

Figure 9. Simulator performance evaluation

339 **5.3.2 Limitations**

- 340 1. The overall computational time for simulation gets increased for a more complex system (multilayer
- 341 tissue models).
- 342 2. The primary function of a game engine is to develop games. The human anatomy is too complex to
- 343 precisely be simulated by a game or physics-based engine.

344 **5.4 HTC Vive as a Surgical Trainer**

345 Many studies have shown that virtual simulators are not very accurate and consistent and even do not

346 provide realistic force or haptic feedback. These high-fidelity VR simulators also have a significant

347 drawback: their high cost. In addition, hardware and software maintenance costs significantly more

348 per year. Although these devices substantially affect overall surgical training, their high price can make

349 them an unwanted choice in the presence of other comparatively low-cost resources. The HTC Vive

350 head-mounted display is an affordable option that provides the vibration effect for tactile movement. For

351 our scenario, we have considered that effect as haptic feedback from the system. We have compared our

352 proposed system in terms of price and function with some of the standard commercially available virtual

353 simulators. A comparative cost analysis has been shown in Table 5. Our study has shown that the HTC

354 Vive can act as the most affordable VR-based surgical trainer combined with an open-source game engine

355 with a bit of compromise in performance and feedback functionality.

Table 5. Comparative cost analysis of various virtual simulators

Device	Description / Characteristics	Cost
MIST VR	Advance technology based on surgical practices curriculum	\$16000 - \$25000
	An expanding library of modules	
	Used in suturing, knot-tying, needle passing and stitching	
LAPSIM Essence	Camera and instrument navigation	\$5900
	Coordination	
	Lifting & grasping	
	Fine dissection	
LAP Mentor III	Portable	\$500
	Cost-effective	
	Height adjustable tower	
	Non-haptic	
	Ideal for team training	
Oculus Rift S	Improved optics with vivid colors	\$770
	Peed and comfort	
	Intuitive, realistic precision	
Samsung Odyssey	Inside-Out Tracking	\$500
	High resolution	
	High-end integrated audio	
	Wider field of view	
HTC Vive	Fully immersive	\$399
	Intuitive controls and gestures	
	Realistic haptic feedback	
	Eye relief adjustments	

6 CONCLUSION AND FUTURE IMPROVEMENTS

This research must be seen as a first step toward developing a functional LPN training simulator. In this study we have shown that a soft body of simplex meshes can be efficiently deformed with a low computational cost and high solving speed. A virtual, realistic LPN simulator based on Unity3D is an efficient and cost-effective solution for surgical training. The experiments resulted in a positive feedback from the medical users, who showed more control over the elasticity and force applied during laparoscopic procedure, thus enhancing their personal training experience. Another novelty of this study is using HTC Vive in LPN training, which has not been explored in this field yet.

We propose the following future improvements:

1. To allow a more realistic behavior, further requirements such as boundary limits, constraints, and force feedback for the system must be determined.
2. The organ and related anatomical structures (adhesive constraints, fascia tissues, and ureter) can be mapped from a large set of data using image analysis and segmentation for better anatomical representation.
3. For evaluation purposes, the simulator's proficiency goals can be determined, and proficiency scores can also be calculated for simulated procedures.

REFERENCES

- [1] Siegel, R. L., Miller, K. D., Fuchs, H. E., and Jemal, A. (2022). Cancer statistics, 2022. *CA: a cancer journal for clinicians*, 72(1), 7-33.
- [2] Robson, C. J. (1963). Radical nephrectomy for renal cell carcinoma. *The Journal of urology*, 89(1), 37-42.
- [3] Robson, C. J., Churchill, B. M., and Anderson, W. (1969). The results of radical nephrectomy for renal cell carcinoma. *The Journal of urology*, 101(3), 297-301.
- [4] Clayman, R. V., Kavoussi, L. R., Soper, N. J., Dierks, S. M., Meretyk, S., Darcy, M. D., ... and Long, S. R. (1991). Laparoscopic nephrectomy: initial case report. *The Journal of urology*, 146(2), 278-282.
- [5] C. Huang, "Clinical comparison of laparoscopy vs open surgery in a radical operation for rectal cancer: A retrospective case-control study", *World Journal of Gastroenterology*, vol. 21, no. 48, p. 13532, 2015. Available: 10.3748/wjg.v21.i48.13532.
- [6] A. Kapoor, "Laparoscopic partial nephrectomy: a challenging operation with a steep learning curve", *Canadian Urological Association Journal*, vol. 3, no. 2, p. 119, 2013. Available: 10.5489/cuaj.1042.
- [7] S. Paterson-Brown, "Peer review report 2 on "Virtual reality training in laparoscopic surgery: A systematic review and meta-analysis", *International Journal of Surgery*, vol. 25, p. 189, 2016. Available: 10.1016/j.ijso.2016.03.056.
- [8] J. Mazurek, P. Kiper, B. Cieřlik, and S. Rutkowski, "Virtual Reality in medicine: a brief overview and future research directions", *Human Movement*, vol. 20, no. 3, pp. 16-22, 2019. Available: 10.5114/hm.2019.83529.
- [9] E. Yiannakopoulou, N. Nikiteas, D. Perrea, and C. Tigris, "Virtual reality simulators and training in laparoscopic surgery," *International Journal of Surgery*, vol. 13, pp. 60-64, 2015. Available: 10.1016/j.ijso.2014.11.014.
- [10] A. Gupta, J. Cecil and M. Pirela-Cruz, "A Cyber-Human based Integrated Assessment approach for Orthopedic Surgical Training," *2020 IEEE 8th International Conference on Serious Games and Applications for Health (SeGAH)*, 2020, pp. 1-8, doi: 10.1109/SeGAH49190.2020.9201817.
- [11] F. Borglund, M. Young, J. Eriksson and A. Rasmussen, "Feedback from HTC Vive Sensors Results in Transient Performance Enhancements on a Juggling Task in Virtual Reality", *Sensors*, vol. 21, no. 9, p. 2966, 2021. Available: 10.3390/s21092966.
- [12] G. Lee and M. Lee, "Can a virtual reality surgical simulation training provide self-driven and mentor-free skills learning? Investigation of the practical influence of the performance metrics from the virtual reality robotic surgery simulator on the skill learning and associated cognitive workloads", *Surgical Endoscopy*, vol. 32, no. 1, pp. 62-72, 2017. Available: 10.1007/s00464-017-5634-6.
- [13] A. Chaudhary, F. Bukhari, W. Iqbal, Z. Nawaz and M. Malik, "Laparoscopic Training Exercises using HTC VIVE", *Intelligent Automation and Soft Computing*, pp. -1-1, 2019. Available: 10.31209/2019.100000149.

- 408 [14] K. Tanjung, F. Nainggolan, B. Siregar, S. Panjaitan and F. Fahmi, "The Use of Virtual Reality
409 Controllers and Comparison Between Vive, Leap Motion and Senso Gloves Applied in The Anatomy
410 Learning System", *Journal of Physics: Conference Series*, vol. 1542, no. 1, p. 012026, 2020.
411 Available: 10.1088/1742-6596/1542/1/012026.
- 412 [15] Chaudhry, A. H., Bukhari, F., Iqbal, W., Nawaz, Z., and Malik, M. K. (2020). Laparoscopic Training
413 Exercises Using HTC VIVE. *Intelligent Automation and Soft Computing*, 26(1).
- 414 [16] J. Haowen, S. Vimalasvaran, B. Myint Kyaw and L. Tudor Car, "Virtual reality in medical students'
415 education: a scoping review protocol", *BMJ Open*, vol. 11, no. 5, p. e046986, 2021. Available:
416 10.1136/bmjopen-2020-046986.
- 417 [17] I. Soares, R. B. Sousa, M. Petry and A. Moreira, "Accuracy and Repeatability Tests on HoloLens
418 2 and HTC Vive", *Multimodal Technologies and Interaction*, vol. 5, no. 8, p. 47, 2021. Available:
419 10.3390/mti5080047.
- 420 [18] Jinglu Zhang, Yao Lyu, Yukun Wang, Yinyu Nie, Xiaosong Yang, Jianjun Zhang, and Jian Chang.
421 Development of laparoscopic cholecystectomy simulator based on the Unity game engine.
422 In Proceedings of the *15th ACM SIGGRAPH European Conference on Visual Media Production (CVMP '18)*. Association for Computing Machinery, New York, NY, USA, Article 4, 1–9.
423 DOI:https://doi.org/10.1145/3278471.3278474
- 424 [19] J. Fürst, G. Fierro, P. Bonnet, and D. Culler. 2014. BUSICO 3D: building simulation and control
425 in unity 3D. In Proceedings of the *12th ACM Conference on Embedded Network Sensor
426 Systems (SenSys '14)*. Association for Computing Machinery, Memphis, TN, USA, pp. 326-327.
427 DOI:http://dx.doi.org/10.1145/2668332.2668380
- 428 [20] J. Craighead, J. Burke, and R. Murphy, "Using the unity game engine to develop sarge: a case study,"
429 *Proceedings of the 2008 Simulation Workshop at International Conference on Intelligent Robots and
430 Systems (IROS)*, Computer, 2008.
- 431 [21] A. Sagor and A. Das, "Study of an Application Development Environment Based on Unity Game
432 Engine," *International Journal of Computer Science and Information Technology*, vol. 12, pp. 43-62,
433 2020. Available:10.5121/ijcsit.2020.12103.
- 434 [22] M. Borges, A. Symington, B. Coltin, T. Smith and R. Ventura, "HTC Vive: Analysis and Accuracy
435 Improvement," 2018 IEEE/RSJ *International Conference on Intelligent Robots and Systems (IROS)*,
436 Madrid, 2018, pp. 2610-2615, DOI: 10.1109/IROS.2018.8593707.
- 437 [23] D. Qiu, X. Jiang and J. Luo, "Modeling and Simulation of Seafarer Lifesaving Training Management
438 System Based on HTC VIVE", *SSRN Electronic Journal*, 2022. Available: 10.2139/ssrn.4156273.
- 439 [24] General Laparoscopy. (2020). "General Laparoscopy Surgical Procedure Nebraska Patient Education",
440 YouTube [Online]. Available: https://youtu.be/d5pqie3usQI. [Accessed: 22- Jan- 2022].
- 441 [25] F. Yu, Q. Xu and X. Liu, "Impact of Laparoscopic Partial Nephrectomy and Open Partial Nephrectomy
442 on Outcomes of Clear Cell Renal Cell Carcinoma", *Frontiers in Surgery*, vol. 8, 2021. Available:
443 10.3389/fsurg.2021.681835.
- 444 [26] G. Verhoest et al., "Transperitoneal Laparoscopic Nephrectomy for Autosomal Dominant Polycystic
445 Kidney Disease," *Journal of the Society of Laparoendoscopic Surgeons (JSLS)*, vol. 16, no. 3, pp.
446 437-442, 2012. Available: 10.4293/108680812x13462882736178.
- 447 [27] D. Christan, "General algorithms for laparoscopic surgical simulators," *Revista Ingenieria Biomedica*,
448 vol. 4, no. 8, pp. 57-70, 2010.
- 449 [28] K. Qian, J. Bai, X. Yang, J. Pan, and J. Zhang, "Essential techniques for laparoscopic surgery
450 simulation," *Computer Animation and Virtual Worlds*, vol. 28, no. 2, pp. e1724, 2016. Available:
451 10.1002/cav.1724.
- 452 [29] T. Kugelstadt, D. Koschier, and J. Bender, "Fast Corotated FEM using Operator Splitting", *Computer
453 Graphics Forum*, vol. 37, no. 8, pp. 149-160, 2018. Available: 10.1111/cgf.13520.
- 454 [30] M. Romeo, C. Monteagudo, and D. Sánchez-Quirós, "Muscle and Fascia Simulation with Extended
455 Position-Based Dynamics," *Computer Graphics Forum*, vol. 39, no. 1, pp. 134-146, 2019. Available:
456 10.1111/cgf.13734.
- 457 [31] J. Bender, M. Müller, M. Otaduy, M. Teschner, and M. Macklin, "A Survey on Position-Based
458 Simulation Methods in Computer Graphics," *Computer Graphics Forum*, vol. 33, no. 6, pp. 228-251,
459 2014. Available: 10.1111/cgf.12346.
- 460 [32] L. Khan, Y. Choi and M. Hong, "Cutting Simulation in Unity 3D Using Position Based Dynamics
461 with Various Refinement Levels", *Electronics*, vol. 11, no. 14, p. 2139, 2022. Available: 10.3390/elec-

- 463 tronics11142139.
- 464 [33] M. Miles, M. Müller, and N. Chentanez, "XPBD: position-based simulation of compliant constrained
465 dynamics," *Proceedings of the 9th International Conference on Motion in Games*, vol. 33, no. 6, pp.
466 49-54, 2016.
- 467 [34] M. Witt, M. Schumann and P. Klimant, "Real-time machine simulation using cutting force calculation
468 based on a voxel material removal model", *The International Journal of Advanced Manufacturing
469 Technology*, vol. 105, no. 5-6, pp. 2321-2328, 2019. Available: 10.1007/s00170-019-04418-2.
- 470 [35] "SOFA - Simulation Open Framework Architecture", *SOFA*, 2022. [Online]. Available:
471 <https://www.sofa-framework.org/>.
- 472 [36] H. Zhong, X. Chen, W. Shu, and X. Chen, "Research and Development on 3D Simulation Training
473 Evaluation System of Substation Based on Unity3D", *Applied Mechanics and Materials*, vol. 727-728,
474 pp. 987-990, 2015. Available: 10.4028/www.scientific.net/amm.727-728.987.
- 475 [37] G. Wheeler et al., "Virtual interaction and visualisation of 3D medical imaging data with
476 VTK and Unity", *Healthcare Technology Letters*, vol. 5, no. 5, pp. 148-153, 2018. Available:
477 10.1049/htl.2018.5064.
- 478 [38] T. Juin-Ling, "Development of a Low-Cost 3D Interactive VR System using SBS 3D Display,
479 VR Headset and Finger Posture Motion Tracking", *International Journal of Advanced Studies in
480 Computer Science and Engineering*, vol. 5, issue. 8, 2016.
- 481 [39] A. Srivastava, S. Kumar, and M. Zareapoor, "Self-organized design of virtual reality simulator for
482 identification and optimization of healthcare software components" *Journal of Ambient Intelligence
483 and Humanized Computing*, 2018. Available: 10.1007/s12652-018-1100-0.
- 484 [40] A. Vamadevan, L. Konge, M. Staeager and F. Bjerrum, "Haptic simulators accelerate laparoscopic
485 simulator training, but skills are not transferable to a non-haptic simulator: a randomized trial",
486 *Surgical Endoscopy*, 2022. Available: 10.1007/s00464-022-09422-4.
- 487 [41] A. Nemani, W. Ahn, C. Cooper, S. Schwaitzberg and S. De, "Convergent validation and transfer of
488 learning studies of a virtual reality-based pattern cutting simulator," *Surgical Endoscopy*, vol. 32, no.
489 3, pp. 1265-1272, 2017. Available: 10.1007/s00464-017-5802-8.
- 490 [42] R. Mao et al., "Immersive Virtual Reality for Surgical Training: A Systematic Review", *Journal of
491 Surgical Research*, vol. 268, pp. 40-58, 2021. Available: 10.1016/j.jss.2021.06.045.
- 492 [43] G. Sommer et al., "The role of virtual reality simulation in surgical training in the light of COVID-19
493 pandemic", *Medicine*, vol. 100, no. 50, p. e27844, 2021. Available: 10.1097/md.0000000000027844.
- 494 [44] Computed Tomography (CT). (2022). Retrieved 6 February 2022, from
495 <https://www.nibib.nih.gov/science-education/science-topics/computed-tomography-ct>
- 496 [45] "Robotic and Laparoscopic Surgery: Overview » Robotic and Laparoscopic Surgery » Department
497 of Urology » College of Medicine » the University of Florida," Urology.ufl.edu, 2020. [Online].
498 Available: <https://urology.ufl.edu/patient-care/robotic-laparoscopic-urologic-surgery/procedures/>.
- 499 [46] Foundation, B. (2022). blender.org - Home of the Blender project - Free and Open 3D Creation
500 Software. [online] *blender.org*. Available at: <https://www.blender.org/>.
- 501 [47] V. Angelov, E. Petkov, G. Shipkovenski and T. Kalushkov, "Modern Virtual Reality Headsets", 2020
502 *International Congress on Human-Computer Interaction, Optimization and Robotic Applications
503 (HORA)*, 2022, pp. 1-5. Available:10.1109/HORA49412.2020.9152604.